DOI: 10.3901/CJME.2011.03.***, available online at www.cjmenet.com; www.cjmenet.com.cn

Life Prediction Based on Transient Dynamics Analysis of Van Semi-trailer with Air Suspension System

LI Liang*, SONG Jian, HE Lin, ZHANG Mengjun, and LI Hongzhi

State Key Laboratory of Automotive Safety and Energy, Tsinghua University, Beijing 100084, China

Received June 1, 2010; revised January 10, 2011; accepted February, 2011; published electronically February, 2011

Abstract: The early fatigue damage in the van-body of the semi-trailer is often caused by the unique mechanical characteristics and the dynamic impact of the loads. The traditional finite element method with static strength analysis cannot support the fatigue design of van-body; thus, the dynamics analysis should be adopted for the endurance performance. The accurate dynamics model to describe the transient impacts of all kinds of uneven road and the proper system transfer functions to calculate the load transfer effects from tire to van-body are two critical factors for transient dynamics analysis. In order to evaluate the dynamic performance, the dynamics model of the trailer with the air suspension is brought forward. Then the analysis method of the power spectral density (PSD) is set up to study the transient responses of the road dynamic impacts. The transient responses transferred from axles to van-body are calculated, such as dynamic stress, dynamic RMS acceleration, and dynamic load factors. Based on the above dynamic responses, the fatigue life of van-body is predicted with the finite element analysis (FEA) method. Applying the test parameters of the trailer with air suspension, the simulation system with Matlab/Simulink is constructed to describe the dynamic responses of the impacts of the tested PSD of the vehicle axles, and then the fatigue life is predicted with FEA method. The simulated results show that the vibration level of the van-body with air suspension is reduced and the fatigue life is improved. The real vehicle tests on different roads are carried out, and the test results validate the accuracy of the simulation system. The proposed fatigue life prediction method is effective for the virtual design of auto-body.

Key words: van-body, air suspension system, transient dynamics, power spectral density (PSD), life prediction

1 Introduction

In order to realize low cost and lightweight design, the aluminum body and the automatic rivet technology are widely used in van semi-trailer. But the road conditions are obviously different in different areas in China, resulting in serious damage of the cargo[1]. Air suspension is one important technology to improve the cargo safety and to decrease the vibration level of van-body. Because new material and manufacturing technique are involved in trailer design, the fatigue life of van-body is affected. Moreover, the uneven county road with large roughness exists in the transport road system, so the fatigue life prediction requires carefully evaluation with the tested road spectra of typical road conditions.

The transient dynamics based on power spectral density (PSD) analyzing method is efficient to evaluate the random dynamic response of van semi-trailer to road impacts[2]. But it cannot give a method to predict the fatigue life of the van-body with the calculated dynamics response. The dynamic inputs excited by road roughness are random in nature, and can be characterized statistically by PSD analyzing method[3]. Based on the results of PSD analysis, the dynamic loads to the auto-body might be calculated, and then the prediction of fatigue life of key components of the trailer might be accomplished with finite element analysis method[4].

With considering that the air suspension may change the transfer function between the impact of the tire and the supports of the van-body, the system dynamics model with air suspension should be applied in the fatigue life prediction of the van-body[5]. Meanwhile, it is complicated to describe the dynamic road loads of the van-body with a proper way. One effective way is to estimate the spectra of dynamic response parameters through PSD of the road and the frequency response function (FRF) of the vehicle[6]. In order to obtain dynamic impacts of road excitations in time domain, the random phase modulation and the discrete numerical simulation method is used to realize the road surface information[7].

The researches mentioned above have given some useful references to analysis the dynamics characteristic of the van-body on the uneven roads. But the fatigue life design process of van-body with air suspension cannot be developed systemically. In this paper, the fatigue life of the van-body with air suspension system will be predicted

* Corresponding author. E-mail: liangl@tsinghua.edu.cn
This project is supported by National Natural Science Foundation of China (Grant No. 50905092)

through the transient dynamic analysis and the finite element analysis. In section 2, the dynamic simulation model of the semi-trailer, including the air suspension system and the van-body of the semi-trailer, is established. In section 3, the random dynamic responses of the van-body, such as the dynamic stress, dynamic RMS acceleration, and the dynamic load coefficients of key points on the auto-body, are calculated with the proposed dynamic simulation model which is used to evaluate the dynamic impacts on the aluminum van-body. And in section 4, the method to predict the fatigue life of whole van-body is brought forward, based on the calculated random dynamic responses. In section 5, simulated and test results of the dynamic performance are demonstrated. Finally, the fatigue life of van-body is evaluated.

2 PSD Analysis System of Van Semi-trailer

2.1 Simulation process of transient dynamic analysis

The response of random vibration is an important dynamic performance for PSD analysis[3,5]. If linear system is simplified, the spectra of dynamic response parameters may be obtained through PSD of the road and the FRF of the vehicle[6]. The dynamic performance may be evaluated based on the dynamic response. The procedure of the transient dynamic analysis is illustrated as Fig. 1. The statistic parameters in random vibration course may be calculated with ANSYS.

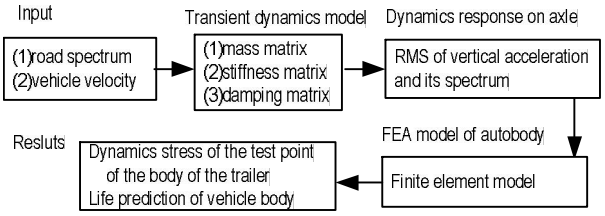

Fig.1. Simulation procedure of transient dynamic analysis

2.2 PSD of road surface

The procedure to establish the random road surface is illustrated as Fig. 2. The road roughness may be expressed as statistic characteristics of the displacement spectrum density of road[8].

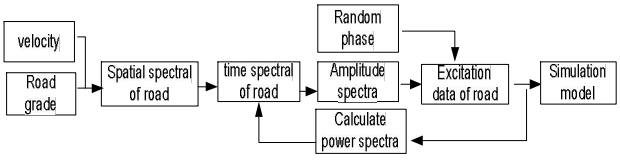

Fig. 2. Procedure to establish the random road surface

According to ISO/TC108/SC2N67, the PSD of road surface may be expressed as follows.

PSD of displacement:

$$G_q(f)=\frac{1}{v}G_q(n_0)\times\left(\frac{n}{n_0}\right)^{-2}=G_q(n_0){n_0}^2\frac{v}{f^2}, \tag{1}$$

PSD of velocity:

$$G_{\dot{q}}(f)=(2\pi f)^2G_q(f)=4\pi^2G_q(n_0){n_0}^2v, \tag{2}$$

PSD of acceleration:

$$G_{\ddot{q}}(f)=(2\pi f)^4G_q(f)=16\pi^4G_q(n_0){n_0}^2vf^2, \tag{3}$$

where $f=nv$, f is time frequency, n is spatial frequency, $n_0=0.1/\mathrm{m}$, v is speed.

The acceleration root mean square(RMS) can be deduced by the square root calculation with Eq. (3)[8]. The rational function is used to express the PSD of the road surface, and the expression of the PSD on the road with rational function is as follows[9]:

$$G_q(n)=\frac{2\alpha\rho}{\pi(\alpha^2+n^2)}, \tag{4}$$

where $G_q(n)$ is a rational function of PSD on the road surface, where α and ρ are constants. Considering the PSD of the road roughness at the same random process can be expressed as Eq. (1) and Eq. (4), α and ρ may be calculated with the least square method:

$$f(\alpha,\rho)=\sum_{f_{\min}}^{f_{\max}}\left[\frac{2\alpha\rho}{\pi(\alpha^2+n^2)}-G_q(n_0)\left(\frac{n}{n_0}\right)^{-2}\right]^2. \tag{5}$$

The constraint conditions are as follows: $\alpha\geq c_1$ and $\rho\geq c_2$; ordinarily, c_1 and c_2 are equal to 0. The values of the constants are listed in Table 1[10].

Table 1. Values of α and ρ

Road roughness level	Constant α/m^{-1}	Constant ρ/m	Speed $v/(\mathrm{km}\cdot\mathrm{h}^{-1})$
A	0.132 0	0.001 5	80
B	0.130 3	0.003 2	45
C	0.120 0	0.006 0	30
D	0.100 7	0.011 5	20

$G_q(n)$ is difficult to obtain directly via the road roughness measurement. But the acceleration can be measured easily; and road roughness may be deduced from the acceleration signals. Then the PSD of road surface may be deduced indirectly with that of the axle. Firstly, the acceleration sensors are installed on the support plates of the axle to measure the acceleration $a(t)$. Thus, $G_a'(f)$ is deduced from a(t) by spectrum analysis. With the vehicle velocity as expressed in Eq.(1), $G_a'(f)$ can be transferred into $G_a'(n)$. Defining $H(f)$ to represent the transfer function from wheel to axle, dynamic characteristics of wheel may be expressed as

$$G_a(f)=H(f)G_a'(f), \tag{6}$$

where $G_a(f)$ is acceleration power spectra of road surface; $H(f)$ is transfer function which can be recognized by frequent weeping test with vibration test bench.

In order to obtain the accurate analysis results, the PSD of axles measured by sensors might be directly used for the dynamics analysis of the trailer. Supposing that the vehicle runs in a straight even ground, the only load is the vertical excitation from the road. In order to get the vibration excitation input for the finite element model of the trailer body, the vertical and the angular vibrations of the sprung mass are changed into the vertical vibration of the support plate on the front or rear axle[6]. Based on the random vibration analysis results of ANSYS, the transient vibration response of van-body structure could be obtained from $G_a(f)$. In order to achieve exact dynamic impacts on van-body from air suspension system, the PSD of road surface is substituted by the PSD of the axle.

2.3 Deduce the input PSD of the axles

The input of PSD of the dual-axles semi-trailer is given as follows. The schematic diagram is illustrated in Fig. 3. $x(I)$ and $y(I)$ are road roughness of the left and right wheel trace, respectively; I is the longitudinal displacement of the trailer. $G_{xx}(n)$ and $G_{xy}(n)$ are self-power spectra and cross-power spectra of $x(I)$, respectively; $G_{yy}(n)$ and $G_{yx}(n)$ are self-power spectra and cross-power spectra of $y(I)$, respectively. The road roughness of four wheels are $q_1(I)$, $q_2(I)$, $q_3(I)$, and $q_4(I)$, respectively. L_s is the distance from towing plate to the front axle of the sub-frame; d is the distance between the front axle and rear axle of the sub-frame.

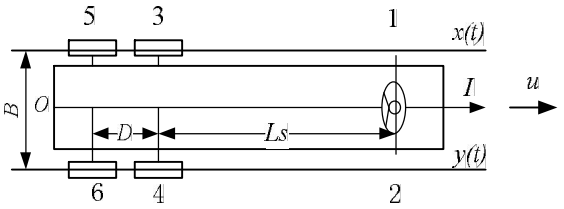

Fig. 3. Schematic diagram of the semi-trailer

Supposing $q_1(I)=x(I)$, $q_2(I)=y(I)$, $q_3(I)=x(I-L_s)$, $q_4(I)=y(I-L_s)$, $q_5(I)=x(I-L_s-d)$, and $q_6(I)=y(I-L_s-d)$, 36 spectra (6 self-power spectra, 30 cross-power spectra) are used to analyze 6 vibration inputs of the trailer, in which 30 cross power spectra are composed of 15 conjugate pairs. The power spectra are expressed as follows [11]:

$$G_{ij}(n)=\lim_{T\to\infty}\frac{1}{T}F_i(n)\overline{F}_j(n), \tag{7}$$

where T is the analysis zone of the longitudinal displacement I. $F_i(n)$ is Fourier transform results of the road roughness. When $F_i(n)$ is at the points of towing plate, the front or rear axles of the trailer are as follows:

$$\begin{cases} F_1(n)=F[q_1(I)]=F[x(I)]=X(n), \\ F_2(n)=F[q_2(I)]=F[x(I-L_s)]=X(n)\exp(-\mathrm{j}2\pi nL_s), \\ F_3(n)=F[q_3(I)]=F[y(I)]=Y(n), \\ F_4(n)=F[q_4(I)]=F[y(I-L_s)]=Y(n)\exp(-\mathrm{j}2\pi n(L_s+d)), \\ F_5(n)=F[q_5(I)]=F[y(I-L_s-d)]=Y(n), \\ F_6(n)=F[q_6(I)]=F[y(I-L_s-d)]=Y(n)\exp(-\mathrm{j}2\pi n(L_s+d)). \end{cases} \tag{8}$$

where $F[x(I)]$ and $F[y(I)]$ are the Fourier transform results of $x(I)$ and $y(I)$ respectively, which can be expressed as $X(n)$ and $Y(n)$.

The statistical property of the roughness of two wheel marks may be expressed by the cross-power spectra[11], and their exponential form is as follows:

$$G_{xy}(n)=|G_{xy}(n)|\exp(\mathrm{j}\phi_{xy}(n)), \tag{9}$$

where $|G_{xy}(n)|$ is the amplitude of the cross-power spectra of $x(I)$ and $y(I)$. $\phi_{xy}(n)$ is the phase spectrum accordingly. When the velocity is lower, like 10 km/h, the wavelength of the road surface irregularity which causes resonance of the vehicle lateral inclination angle was very short, the coherence spectrum was depressed to 0.1. The correlation of the left and right wheel trace road was low. Input force of vehicle lateral inclination angle vibration was much larger than that of vertical vibration. If the coherence spectrum was about 0.9, the vertical vibration input force became primary and important. Based on the test, the average phase difference was similar to zero. Supposing the statistic property of the road roughness of the left wheel mark and the right wheel mark are similar, $G_q(n)=G_{xx}(n)=G_{yy}(n), \phi_{xy}(n)=0$, then

$$G_{yx}(n)=G_{xy}(n)=C_{xy}(n)G_q(n), \tag{10}$$

and the coherence function is

$$C_{xy}^2(n)=\frac{\left|G_{xy}(n)\right|^2}{G_{xx}(n)G_{yy}(n)}. \tag{11}$$

Supposing $x(I)$ and $y(I)$ complete linear correction, the input matrix of PSD of semi-trailer is expressed as follows:

$$(G_{ij}(n))_{6\times6}=G_q(n)\times$$
$$\begin{pmatrix}
1 & C(n) & \exp(-\mathrm{j}2\pi nL_s) \\
C(n) & 1 & C(n)\exp(-\mathrm{j}2\pi nL_s) \\
\exp(\mathrm{j}2\pi nL_s) & C(n)\exp(\mathrm{j}2\pi nL_s) & 1 \\
C(n)\exp(\mathrm{j}2\pi nL_s) & \exp(\mathrm{j}2\pi nL_s) & C(n) \\
\exp(\mathrm{j}2\pi n(L_s+d)) & C(n)\exp(\mathrm{j}2\pi n(L_s+d)) & \exp(\mathrm{j}2\pi nd) \\
C(n)\exp(\mathrm{j}2\pi n(L_s+d)) & \exp(\mathrm{j}2\pi n(L_s+d) & C(n)\exp(\mathrm{j}2\pi nd)
\end{pmatrix}$$
$$\begin{pmatrix}
C(n)\exp(-\mathrm{j}2\pi nL_s) & \exp(-\mathrm{j}2\pi n(L_s+d)) & C(n)\exp(-\mathrm{j}2\pi n(L_s+d)) \\
\exp(-\mathrm{j}2\pi nL_s) & C(n)\exp(-\mathrm{j}2\pi n(L_s+d)) & \exp(-\mathrm{j}2\pi n(L_s+d)) \\
C(n) & \exp(-\mathrm{j}2\pi nd) & C(n)\exp(-\mathrm{j}2\pi nd) \\
1 & C(n)\exp(-\mathrm{j}2\pi nd) & \exp(-\mathrm{j}2\pi nd) \\
C(n)\exp(\mathrm{j}2\pi nd) & 1 & C(n) \\
\exp(\mathrm{j}2\pi nd) & C(n) & 1
\end{pmatrix}. \tag{12}$$

In the simulation system with ANSYS, cross-power spectra may be solved by the real part and the imagine part respectively, which are unified into a single spectrum. Thus, Eq. (12) may be simplified as follows:

$$(G(f))=\begin{pmatrix}
G_{11}(f) & C_{12}(f)+iQ_{12}(f) & C_{13}(f)+iQ_{13}(f) \\
C_{12}(f)-iQ_{12}(f) & G_{22}(f) & C_{23}(f)+iQ_{23}(f) \\
C_{13}(f)-iQ_{13}(f) & C_{23}(f)-iQ_{23}(f) & G_{33}(f)
\end{pmatrix}, \tag{13}$$

where, $G_{ii}(n)=G_q(n)$, $G_{ij}(f)=\cos(2\pi fL_{sij}/v)$, $Q_{ij}(f)=\sin(2\pi fL_{sij}/v)$ (i, j=1, 2,⋯, m). L_{sij} is the distance between points i and j. $(G(f))$ is an anti-symmetric matrix, where needs (m^2-m) cross-power spectra curves and m self-power spectra curves to calculate $(G(f))$. If the input spectra of left and the right wheels are equal, the trailer model might be simplified into one side model; thus, m=3. Therefore, only 9 spectra curves are required.

3 Transient Dynamic Analysis Model

3.1 Model of vehicle with air suspension

5 DOFs dynamic model of the trailer with air suspension system is illustrated as Fig. 4. The nomenclatures in Fig. 4 are listed in Table 2.

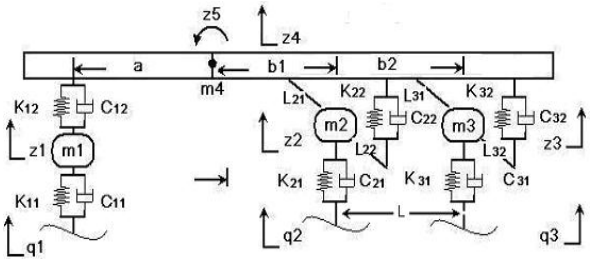

Fig. 4. Air suspension model of van semi-trailer

In the low-frequency range, the attenuation of the tire damping to dynamic loads is not obvious. But attenuation effect becomes obvious as excitation frequency increases. For the conservative design of air suspension, the tire damping may be supposed as zero ($(\dot{Q})=0$). Thus, Eq. (23) may be expressed as state space equation for the application in the simulation system:

$$\begin{cases}\dot{\boldsymbol{x}}=\boldsymbol{A}\boldsymbol{x}+\boldsymbol{B}\boldsymbol{u}, \\ \boldsymbol{y}=\boldsymbol{C}\boldsymbol{x}+\boldsymbol{D}\boldsymbol{u}.\end{cases} \tag{14}$$

Where

$$\boldsymbol{A}=\begin{pmatrix}\boldsymbol{0} & \boldsymbol{I} \\ -\dfrac{\boldsymbol{K}}{\boldsymbol{M}} & -\dfrac{\boldsymbol{C}}{\boldsymbol{M}}\end{pmatrix},$$
$$\boldsymbol{B}_{3\times10}=\begin{pmatrix}
0 & \cdots & 0 & \dfrac{k_{11}}{m_1} & 0 & 0 & 0 & \cdots & 0 \\
0 & \cdots & 0 & 0 & \dfrac{k_{21}}{m_2} & 0 & 0 & \cdots & 0 \\
0 & \cdots & 0 & 0 & 0 & \dfrac{k_{31}}{m_3} & 0 & \cdots & 0
\end{pmatrix},$$
$$\boldsymbol{x}=(z_1\ z_2\ z_3\ z_4\ z_5\ \dot{z}_1\ \dot{z}_2\ \dot{z}_3\ \dot{z}_4\ \dot{z}_5)^{\mathrm{T}},$$
$$\boldsymbol{u}=(q_1\ q_2\ q_3)^{\mathrm{T}}.$$

$\boldsymbol{x}$ is state vector of the trailer, 10 states include 5 DOFs of displacement and 5 DOFs of velocity of the trailer, $\boldsymbol{u}$ is the excitation vector to the wheel; $\boldsymbol{y}$ is the output vector; **A** is the system matrix; $\boldsymbol{C}$ is the output matrix; $\boldsymbol{D}$ is the zero matrix.

Table 2. Dynamics parameters of the trailer

Parameter	Value
Sprung mass m_4/kg	24 227
Moment of inertia of sprung mass m_5/(kg • mm)	0.399×10^{12}
Unspung mass m_1/kg	1 260
Sprung mass of front axle m_2/kg	1 260
Unsprung mass of front axle m_3/kg	1 260
Vehicle front suspension stiffness k_{12}/(N • mm^{-1})	900
Trailer front suspension stiffness k_{22}/(N • mm^{-1})	360
Stiffness of rear suspension k_{32}/(N • mm^{-1})	360
Vehicle front suspension damping c_{12}/(N • s • mm^{-1})	$0.032k_{12}$
Trailer front suspension damping c_{22}/(N • s • mm^{-1})	$0.12k_{12}$
Trailer rear suspension damping c_{32}/(N • s • mm^{-1})	$0.12k_{12}$
Length of rear beam L_{21}, L_{22}/mm	380
Sum of vehicle front stiffness k_{11}/(N • mm^{-1})	12 046
Sum of trailer front tires stiffness k_{21}/(N • mm^{-1})	12 046
Sum of trailer rear tires stiffness k_{31}/(N • mm^{-1})	12 046
Vehicle front wheels damping c_{11}/(N • s • mm^{-1})	1.4
Trailer front wheels damping c_{21}/(N • s • mm^{-1})	2.4
Trailer rear wheels damping c_{31}/(N • s • mm^{-1})	2.4
Length between two axle L/mm	1 360
Length between front axle and gravity center(GC) of the trailer a/mm	5 799
Length between rear axle and GC b_1/mm	2 847
Length between front axle and GC b_2/mm	4 207
Length of front beam L_{31}, L_{32}/mm	500

3.2 PSD model of the trailer with air suspension

The sketch of the simulation model for PSD analysis developed by Matlab/Simulink is illustrated in Fig. 5. In order to validate this model, a real trailer with 24 strain test points and 20 acceleration test points is developed, which may be illustrated in Fig. 6.

With the simulation system, the time-history of the vertical acceleration and the acceleration RMS are

calculated, and then the dynamic responses at key points are deduced. The random vibration analysis is processed with ANSYS to calculate the dynamic response of the same key points on the structure of the trailer.

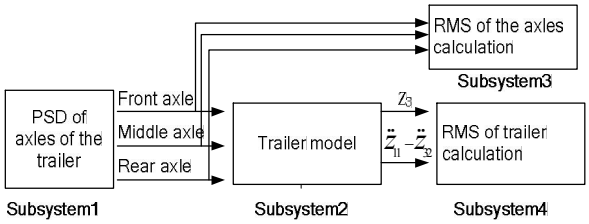

Fig. 5. Simulation model for the transient dynamic analysis

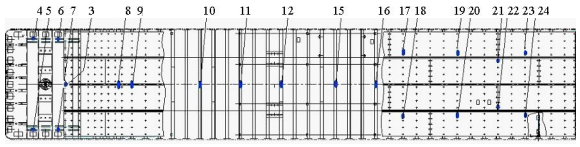

(a) Test points of strain on the bottom frame of auto-body

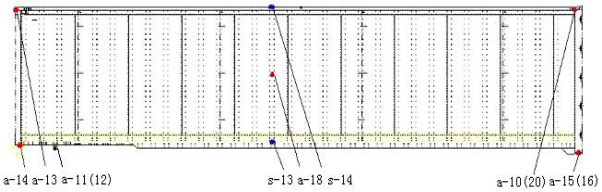

(b) Test points of strain and acceleration on side plate (a denotes acceleration test points, s denotes strain test points)

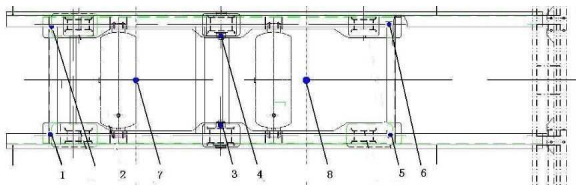

(c) Test points of acceleration on the bottom plate of auto-body

Fig. 6. Schematic diagram of the strain test points and the acceleration test points

The simulation test conditions are as follows: the trailer load is fully loaded, 20 t; the road grades are highway, level A, level B, and level C. The measured PSD of the axles are used to substitute the PSD of the road. The time-histories of the strain and acceleration are measured. The strain test points are selected for two reasons: firstly, the points with extreme stress and displacement in the simulation results are selected; secondly, the points at which the stress concentration may be damaged easily in the service period. From the measured data, the displacement, the velocity, the acceleration, and the PSD of dynamic stress ($G_\sigma(f)$) are deduced. The acceleration tests points are placed on the connection point of the tractor pin, the support plates of front and rear axles, and the support plates on the tractor axel.

3.3 Finite element analysis(FEA) model of the trailer

The FEA model for the dynamic analysis and the fatigue life prediction was set up, as illustrated in Fig. 7. The beam element is used to simplify the solid model for the grid component of the suspension system. The mass element is used to simulate the unload parts of the body. The bottom plate and beam are fixed by the bolts, and then the plane degrees of freedom at the connection key points are constrained. The side plates are constructed with the aluminum plate, and connected by the rivet joints. The elastic-plastic shell elements are used for the body, considering that the body is connected by the rivet joints. And then the joints are coupled or merged. Thus, the stiffness of the model may be increased.

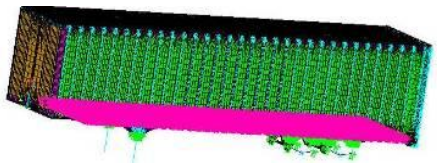

Fig. 7. FEA model of the van-body

3.4 Fatigue life prediction model with FEA

The stochastic fatigue life prediction can be accomplished with FEA model. In the field of engineering, the fatigue calculation method is used with the nominal stress extensively. Thus, the fatigue life is estimated by the S-N curve. Because the stress course is a random course, the calculation of fatigue life is complicated. The linear cumulative damage rule assumes that the total life of a structural part can be predicted by merely adding up the percentage of life consumed by each stress cycle[13]. For the fatigue life calculation, RMS stress quantities deduced from the PSD analysis are used in conjunction with the standard fatigue analysis procedure. According to Palmgren-Miner linear cumulative damage rule for the narrow-band random vibrations, the fatigue life prediction procedure is listed as follows[14]. The expected damage due to the number of fatigue peaks, when the random stress course $\sigma(t)$ lies in a narrow-banded random at time T, which is given by

$$D(s)=\frac{n(s)}{N(s)}, \tag{15}$$

where $n(s)$ is the number of cycles occurring at the considered stress level and the number of allowable cycles $N(s)$ is taken from the S-N curve, in general, described by the following equation:

$$N(s)=\frac{C}{s^m}, \tag{16}$$

where C, m are material fatigue experiment constants.

Because the spectral content is a narrow-band process, the cumulative damage can be calculated as [15]

$$D(s)=\frac{n(s)}{N(s)}=\frac{v_0^+T}{C}\{\sqrt{2}\sigma_y\}^b\Gamma\left(1+\frac{b}{2}\right), \tag{17}$$

where $\Gamma(x)=\int_0^{\infty}t^{x-1}\exp(-t)\,\mathrm{d}t$, $v_0^+=\sigma_{\dot{y}}/\sigma_y$, σ_y and $\sigma_{\dot{y}}$ represent the RMS value and velocity RMS of the induced stress component. Assuming that the available cumulative damage is $D(s)\approx1$ when van-body fails due to fatigue, the expected life time T_a can be calculated as[4]

$$T_a=2^{1-m/2}\pi C\sigma_{\dot{y}}{}^{-1}\sigma_y{}^{1-m}\Gamma^{-1}\left(\frac{m}{2}+1\right). \tag{18}$$

Finally, accumulated mileage of the trailer can be calculated as

$$T_a'=\frac{T_a}{60}. \tag{19}$$

4 Transient Dynamic Analysis

4.1 PSD and displacement of axle

The tested accelerating PSD curve is illustrated in Fig. 8. And the displacement RMS deduced from Eq. (3) is listed in Table 3[10]. As listed in Table 3, the axle displacements are similar to the values of the reference road. But the four curves of the displacement RMS differentiate at low frequency, ranging from 1 Hz to 2 Hz. The tested data are used in the simulation to evaluate the performance of the air suspension system on the road, and the simulated results are compared with the tested ones directly.

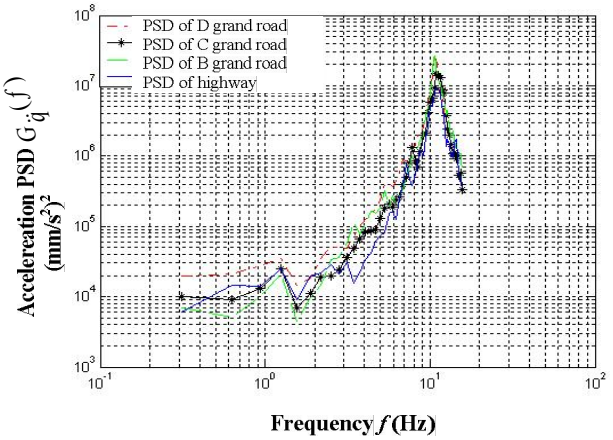

Fig. 8. Acceleration PSD of the axle on different roads

Table 3. Displacement RMS of the trailer axle m

Road grand	Front axle	Rear axle	Reference value
Highway	0.0084	0.0057	0.0058
B grand road	0.3401	0.0118	0.0115
C grand road	0.0394	0.0315	0.0231
D grand road	0.0482	0.0320	0.0462

The transient responses of the key points are listed in Table 4, where T denotes tested value, S denotes simulated value. Most of the simulated and tested results of the acceleration RMS are similar, which means the simulation model is acceptable to simulate the PSD of road surface. The errors are mainly caused by the reason that the PSD of road is too complicated to obtain exactly equal signals from the test process for the simulation analysis. With the displacements of the axles, the boundary conditions of the key nodes of the FEA model could be determined by the displacements PSD. The five key nodes are four supporting points above the axles of the trailer and one supporting point of the tractor pin. The dynamic response to the displacement, stress, and strain may be calculated with the dynamic load of the acceleration PSD.

Table 4. Acceleration RMS

Different test points	Acceleration response result a_{rms}/(m • s^{-2})					
	A grand (60 km/h)		B grand (45 km/h)		C road (30 km/h)	
	T	S	T	S	T	S
Above suspension	1.38	0.76	1.34	1.13	1.17	1.39
Under suspension	6.93	5.85	6.10	8.41	7.12	10.7
Above front suspension	0.75	0.50	0.79	0.70	0.82	0.91
Under front suspension	6.93	5.16	6.10	7.13	7.13	8.83
Above rear suspension	0.79	0.55	0.86	0.79	0.87	1.02
Under rear suspension	6.57	5.14	5.99	7.13	7.48	8.81
Road roughness RMS R_a	3.81	4.34	7.61	7.26	15.2	10.7

4.2 Dynamic stress and PSD of test points

The curves of the simulated dynamic stress σ are plotted with the dynamic stress, as illustrated in Fig. 9. The tested PSD of the dynamic stresses of the key point 12 are plotted as illustrated in Fig. 10. As shown in Fig. 10, the shapes of the curves are similar. And the values of the PSD of the dynamic stresses and the tested stresses are consistent with the variations.

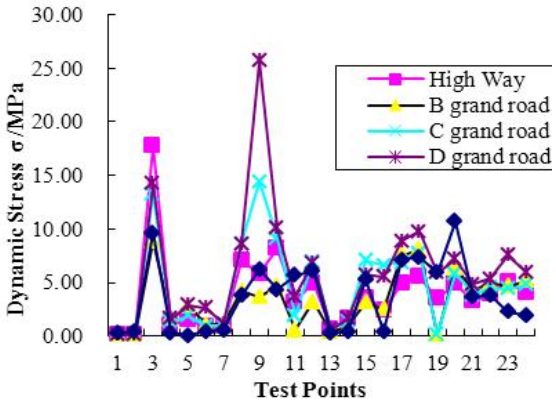

Fig. 9. Simulated dynamic stress results of test points with acceleration PSD input

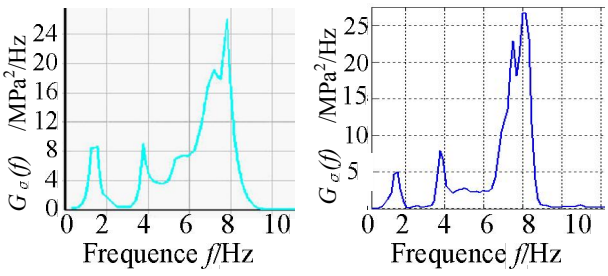

Simulation results of key point 12　　Test results of key point 12

Fig. 10. Simulation and test results of dynamic stress PSD

4.3 Dynamic stress PSD and dynamic load factor

Both point 8 and point 12 are selected to analyze the response of the dynamic stress PSD. The tested results and the simulated results are similar and the curves are consistent with the variation. The peak values appear at the frequency of 1.6 Hz, 3.75 Hz, and 7.81 Hz. The first frequency is corresponding to the vertical vibration mode, which is the main excitation mode; the second one is corresponding to the first torsion mode of the trailer body; and the third one is corresponding to the second mode of the bending deformation of the side plates and frame of auto-body. These three modals are excited during the road test. The dynamic load factors (ratio of dynamic stress and static stress) at the selected points are listed in Table 5. The values vary from 1.2 to 1.8, corresponding to that at the high stress points, such as point 3, point 8, and point 12. But the dynamic coefficients could be larger than that at point 3 when the stresses on the points are small. The simulated dynamic factors are larger than that at point 2, when the trailer is in a transient impact process in a velocity of 10 km/h.

Table 5. Results of dynamic load factor

Key point	1st grand road		2nd grand road		3rd grand road	
	Min	Max	Min	Max	Min	Max
3	0.67	1.37	0.76	1.24	0.19	1.72
8	1.47	0.64	1.58	0.43	1.88	0.14
12	1.26	0.83	1.53	0.50	1.68	0.14
13	2.55	−0.56	3.70	−2.30	8.26	−3.11
14	−0.65	2.41	−1.57	3.93	−3.14	6.12
20	0.83	1.22	0.81	1.16	0.73	1.25

4.4 Acceleration RMS and PSD

The simulated results of the dynamic acceleration RMS are illustrated in Fig. 11. The acceleration RMS are in the range of 550–750 mm/s^2 on the A grand road, and the top values will reach 1 200 mm/s^2 at the middle part of the trailer frame; the values are in the range of 650–850 mm/s^2 on the C grand road, and the top values will reach over 1900 mm/s^2 at the middle part of the frame. The accelerations PSD at two key points are figured in Fig. 12. The simulated results are consistent with the tested ones; key point 3 is near the front support plate. The tested and the simulated results are close and the curves are consistent with the variation.

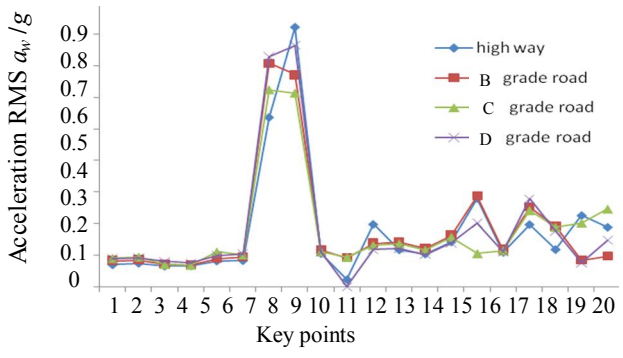

Fig. 11. Simulation values dynamic acceleration RMS

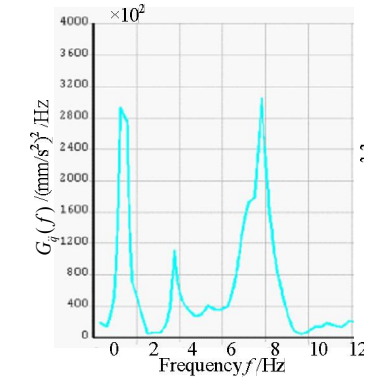

(a) Simulation results of key point 3

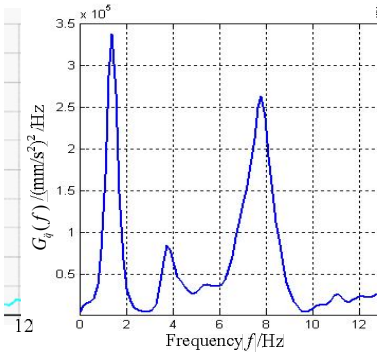

(b) Test results of key point 3

Fig. 12. Simulation and test results of acceleration PSD

4.5 Fatigue life prediction results

Based on PSD analysis of the random response, dynamic stress of the van-body may be calculated. Then the fatigue life can be predicted with ANSYS, the random fatigue life is calculated, and the damaged positions could be recognized. And the positions require to be strengthened are listed in Table 6.

Table 6. Fatigue life for the 3rd grand road

Test point	Dynamic stress σ/MPa	Velocity of dynamic stress $\dot{\sigma}$ /(MPa • s^{-1})	Acceleration of dynamic stress $\ddot{\sigma}$ /(MPa • s^{-2})	Fatigue life T_a'/km
3	15.58	261.87	12 033.51	3.49×10^9
17	58.04	621.93	11 336.28	3.12×10^6
18	59.72	639.87	11 736.61	2.65×10^6
19	19.65	256.37	8 040.35	1.20×10^9
20	20.43	264.45	8 276.09	9.71×10^8
23	21.49	258.72	6 161.52	7.84×10^8
24	21.10	256.39	6 284.72	8.62×10^8

The RMS nominal stresses of the tested points, such as point 3 on the bottom plate, points 17, 18, 19, 20, 23 and 24 on the bottom frame, are larger than those on the other parts of the van-body. The early fatigue could be induced by the stress concentration and the van-body may be damaged from these points. The fatigue life in the cloud images reflects the fracture as illustrated in Fig. 13. The beams above the front and rear supports of the bottom frame are fragile, which can be easily damaged by the dynamic loads from the suspension, as illustrated in Fig. 13(a). Meanwhile,

the support of the towing device needs to be strengthened, as illustrated in Fig. 13(b).

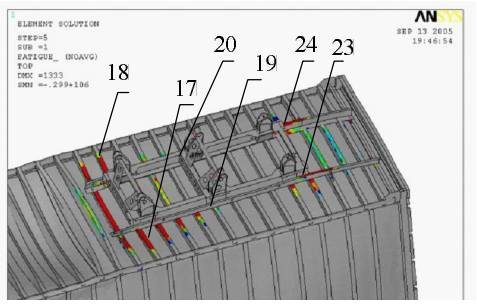

(a) Fatigue life of the bottom beam

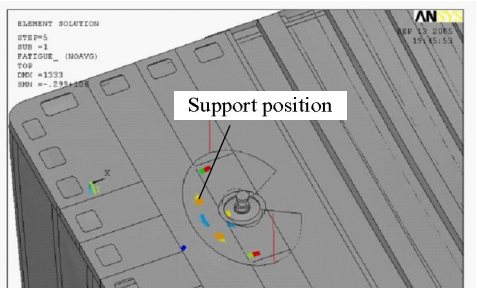

(b) Fatigue life of the supports

Fig. 13. Fatigue life of the van-body of trailer

5 Conclusions

(1) The transient dynamic analysis model, based on the PSD, is brought forward to simulate the responses of the trailer with the air suspension system. The vibration excitations of the key points on the support plates of the van-body are deduced with the simulation model. Moreover, the dynamic stress traces at the key points of the van-body are obtained with full finite element model.

(2) The fatigue life of the van-body is predicted with the results of PSD analysis and fracture positions are recognized, so the key parameters of the suspension system and the material of the key positions of the van-body can be changed to improve the fatigue life.

(3) The results of the fatigue experiment are consistent with the ones obtained from the simulation system. It proves that the simulation model for the transient dynamic analysis and fatigue life prediction work very well. Therefore, the system might be built to provide practical suggestions for the air suspension design for the van semi-trailer.

References

[1] PALKOVICS L, FRIES A. Intelligent electronic systems in commercial vehicle for enhanced traffic safety[J]. *Vehicle System Dynamic*, 2001, 35(4–5): 227–289.

[2] GILLESPIE T D. *Fundamentals of vehicle dynamic*[M]. Warrendale: Society of Automotive Engineers, 1992.

[3] WATERS T P, HYUN Y, BRENNAN M J. The effect of dual-rate suspension damping on vehicle response to transient road input[J]. *Journal of Vibration and Acoustics, ASME*, 2009, 131(2): 1–7.

[4] ZHANG Mengjun, WANG Huiyi, LI Liang, et al. FEM study for van trailer dynamic performance with air suspension[G]. *SAE Paper*, 2006-01-3521, 2006.

[5] YANG Yong, REN Weiqun, CHEN Liping, et, al. Study on ride comfort of tractor with tandem suspension based on multi-body system dynamic[J]. *Applied Mathematical Modelling*, 2009, 33(1): 11–33.

[6] WIESAW Bereś. Ride dynamic modeling of mining bucket loaders[J]. *Vehicle System Dynamic*, 1998, 17(S1): 49–52.

[7] ANDREN P. Power spectral density approximations of longitudinal road profiles[J]. *International Journal of Vehicle Design*, 2006, 40(1–3): 2–14.

[8] HOU Xiangshen, SHAN Liyan, MA Songlin. Influence of pavement roughness on riding comfort based on whole vehicle model[C]// *International Conference on Transportation Engineering*, Chengdu, China, 2007: 655–662.

[9] ALEXANDRU N D. Spectral shaping for codes with P.S.D. expressed by rational functions[C]//*The 9th International Conference on Development and ApplicationSystem,* Suceava, Romania, 2008: 31–35.

[10] China State Bureau of Standards. *GB 7031-86 Expression way of road roughness for input of vehicle vibration*[S]. Beijing: China Standard Press, 1986. (in Chinese)

[11] BENDAT J S, PIERSOL A G. *Random data: analysis and measurement procedures*[M]. New York, Wiley, 1966.

[12] HEAVY J W. Truck suspension dynamic methods for evaluating suspension road friendliness and ride qualityG]. *SAE Paper*, 962152, 1996.

[13] STEINBERG D S. Quick way to predict random vibration failures[J]. *Machine Design*, 1978, 50(8): 188–191.

[14] JIAO G, MOAN T. Probabilistic analysis of fatigue due to Gaussian load process[J]. *Probabilistic Engineering Mechanics*, 1990, 5(2): 76–83.

[15] WIJKER J J. Spacecraft structures[M]. Berlin: Springer, 2008.

Biographical notes

LI Liang is currently a research assistant in mechanical engineering of *Tsinghua University, China*. His research interests include vehicle dynamics and control, vehicle system simulation and controller development. He received his PhD from *Tsinghua University, China*, in 2008.
E-mail: liangl@tsinghua.edu.cn

SONG Jian is a professor in *Tsinghua University, China*. He is the vice director of *State Key Laboratory of Automotive Safety and Energy, Tsinghua University, China*. His current research interests include vehicle dynamics and control, vehicle CAE. He received his PhD from *Tsinghua University, China*, in 1990.

HE Lin is currently a post-doctor in *Tsinghua University, China*. His research interests include vehicle electronic and control. He received his PhD from *Tongji University, China*, in 2009.

ZHANG Mengjun is a master in *Tsinghua University, China*. He currently works at Pan Asia Technical Automotive Center Co. Ltd., and his research interest includes vehicle body design and road test.

LI Hongzhi is currently a doctoral candidate in *Tsinghua University, China*. His research interests include vehicle dynamics and vehicle electronic control.